IAC-15.B5.1.9

MONITORING THE GLOBAL ASTEROID IMPACT RISK

Clemens Rumpf,

University of Southampton, Faculty of Engineering and the Environment, UK, c.rumpf@soton.ac.uk

Hugh G. Lewis[*], Peter M. Atkinson[†‡§**]

ESA's asteroid risk list contains all known asteroids that have a non-zero chance of colliding with the Earth in the future. The possible impact locations of the asteroids in the list with a minimum diameter of 30 m were calculated. To this end, the freely available software OrbFit was utilized to find orbit solutions for each asteroid that result in a future collision with the Earth. These orbit solutions are called virtual impactors (VIs). Subsequently, the Asteroid Risk Mitigation Optimization and Research (ARMOR) tool was used to determine the impact locations for each VI taking into account orbit solution uncertainty and global impact probability. The resulting 261 impact corridors were visualized on a global map. Furthermore, the impact data were combined with Earth population data to determine the risk of direct asteroid impacts that each nation faces until 2100. These data are the global asteroid risk distribution based on observed asteroids as is known today. A ranking of the countries that exhibit highest risk was produced showing their relative risk with respect to the global risk. It becomes clear that population size is a good proxy for relative risk. Each nation should raise public awareness about the asteroid hazard and should include the asteroid threat in their natural disaster response planning. Physical impact effects are introduced into the analysis. This expands the validity of the results beyond the previously considered relative risk and allows the estimation of the future absolute risk (expected casualties) that the currently known asteroids pose to the populations of the Earth. The alteration of the results based on the introduction of physical impact effects is discussed.

I. INTRODUCTION

Earth has collided with asteroids since it was a planetesimal and this process continues today albeit at a lower rate [1]. Asteroid impacts have been responsible for at least two major disruptions in the evolution of life [2,3] and today, they remain a potential hazard for the human population [4,5]. Surveys scan the sky for asteroids in an effort to discover as many as possible and to calculate their orbits [6]. Based on the propagation of orbits, those asteroids are identified that potentially impact the Earth in the future. The European Space Agency (ESA) and the National Aeronautics and Space Administration (NASA), perform the collision detection using automated systems and the results are published on their respective Near Earth Object (NEO) webpages [7,8]. At the University of Southampton, the Asteroid Risk Mitigation Optimization and Research (ARMOR) tool is under development with the objective of helping to analyse the threat posed by discovered asteroids. Here, the global impact distribution of 69 known asteroids resulting in 261 potential collisions with the Earth was calculated and the result was analysed for the risk distribution on Earth. In particular, the question of how important the introduction of physical impact effects is for the risk distribution as opposed to results that only account for impact location was addressed.

ARMOR can calculate the impact locations of asteroids taking into account their spatial impact probability distribution. This capability allows the determination of the relative risk of direct asteroid impacts that each nation carries. Relative risk is in contrast to "absolute" risk in the sense that "absolute" risk is a statement about how many casualties are expected while relative risk loses this informational content. Instead, relative impact risk allows statements about whether one country faces a higher risk compared to another. This qualification was necessary because ARMOR did not originally account for physical impact effects (such as crater forming, seismic shocks and aerodynamic shock waves) that allow casualty estimation. Additionally, the lack of physical effect modelling constrained the work to the direct asteroid impact scenario –that is, only considering the grid cell for risk analysis, where the impact is predicted- because without the propagation of impact effects it was impossible to determine the region that would be affected by an asteroid impact. The relative risk calculation results were presented at the "2015 Planetary Defense

[*] University of Southampton, Faculty of Engineering and Environment, Southampton, UK, h.g.lewis@soton.ac.uk
[†] Lancaster University, Faculty of Science and Technology , Lancaster, UK, pma@lancaster.ac.uk
[‡] University of Utrecht, Faculty of Geosciences, Utrecht, The Netherlands
[§] University of Southampton, Geography and Environment, Southampton, UK
[**] Queen's University Belfast, School of Geography, Archaeology and Palaeoecology, Belfast, UK

Conference" and the corresponding paper has been published [9].The feedback from the scientific community prompted the question of how much the risk landscape would change with the introduction of physical impact effects. The development of ARMOR has progressed since then and the tool is now able to model impact effects and to estimate the risk of asteroid impacts where the unit of risk is expected casualties. The purpose of this publication is to clarify how much physical impact effects and subsequent casualty estimation influence risk distribution. Does the risk ranking of nations change?

II. METHOD

The processes and method used by ARMOR that leads to the results in this paper is described here. It should be noted that the term "impact" can refer to a general collision between an asteroid and the Earth, an airburst or the event of contact between the asteroid and the surface of the Earth. Where the context requires clarification, the first case is referred to as "collision" the second as "airburst" and the third case as "ground impact".

The method starts with the calculation of the impact location of observed asteroids

II.I IMPACT LOCATION AND PROPABILITY

The nominal orbital solution of an asteroid is a state vector describing the asteroid's orbit and position that fit best the observations that are available for this asteroid. A covariance matrix represents the uncertainty region that is associated with the orbital solution. The uncertainty region has a weak direction, commonly referred to as Line of Variation (LOV), along which the asteroid position is only poorly constrained and it typically stretches along the orbit of the asteroid [10]. Using the data of available observations and the current nominal orbital solution of an asteroid that are provided on the ESA NEO webpage, the freely available software OrbFit [11] was utilized to identify orbit solutions that lie on the LOV as well as inside the uncertainty region and that result in a future Earth impact. OrbFit samples the uncertainty region to find these impacting orbit solutions that are called virtual impactors (VI). It should be noted that one asteroid may have multiple impact possibilities in the future and thus yields more than one VI.

The ARMOR tool was used subsequently to project the impact probability of these VIs onto the surface of the Earth. ARMOR used the VI orbit solution from OrbFit as the initial condition for the trajectory propagation until impact. Each VI propagation was started 10 days before impact and utilized a solar system model that considered gravitational forces from the Sun, the barycenters of the planets (and Pluto) and their satellites as well as point sources for the Earth and the Moon. The positions of the attracting bodies were retrieved from a lookup table that is based on the JPL DE430 planetary ephemerides [12] and the interpolation scheme achieves millimeter level accuracy with respect to HORIZONS. The resulting gravitational acceleration $\ddot{r}$ for the VI is given by:

$$\ddot{r}_j = \sum_{i=1}^{11} -\frac{GM_i}{|r_{ij}|^3} r_{ij} \qquad Eq\ 1$$

where subscript j denotes the VI, subscript i denotes the attracting body, r_{ij} is the position vector connecting the attracting body to the VI and GM_i is the gravitational constant of the attracting body. The gravitational differential equation is numerically solved using the variable time step, predictor-corrector ADAMS method of the Livermore Solver for Ordinary Differential Equations (LSODE) [13] package that is used in the Python *scipy.integrate.odeint* function. Figure 1 shows the position discrepancy of the propagator compared to NASA's HORIZONS system [14] for three asteroids over a 50 day period. In the application presented here, the propagator was used for propagation times of 10 days and the position error remains well bounded to within 50 m in this time frame.

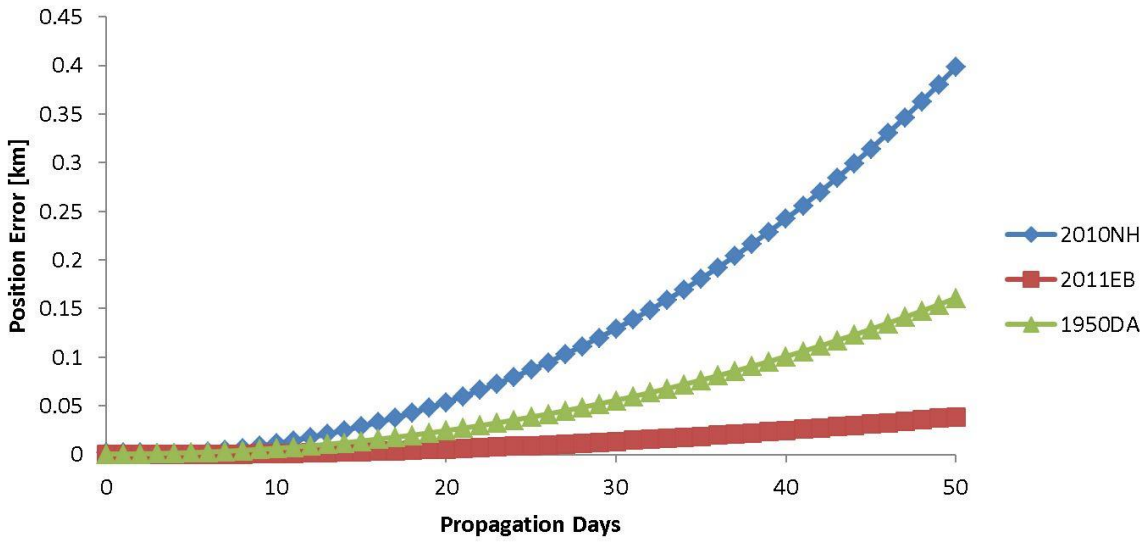

Figure 1: Propagator accuracy comparison with JPL's HORIZONS system for 3 asteroids over a 50 day period. Note that the error does not grow exponentially but shows linear growth with sinusoidal characteristics for longer propagation times.

ARMOR's propagator provides the trajectory of the VI and the Earth as a set of x, y, z coordinate time histories. The approximate impact time and location are determined by comparing the coordinates of the Earth and the VI. In the vicinity of the impact, the trajectories of the Earth and the VI are expressed by three-dimensional polynomials with time as the independent variable, which facilitates determination of impact points in analytical form. The method uses least squares to fit each coordinate component to a third order polynomial of the form:

$$P = c_0 + c_1 t + c_2 t^2 + c_3 t^3 \qquad \textit{Eq 2}$$

For Earth's x component, the expression is:

$$P_{\{\text{♁},x\}} = c_{\{0,\text{♁},x\}} + c_{\{1,\text{♁},x\}}\, t + c_{\{2,\text{♁},x\}}\, t^2 + c_{\{3,\text{♁},x\}} t^3 \qquad \textit{Eq 3}$$

Where $P_{\{\text{♁},x\}}$ is the polynomial expression for the Earth's (♁) x component, $c_{\{0,\text{♁},x\}}$ is one of the polynomial coefficients and t is time as the independent variable. Similarly, the asteroid's $(+)$ x component is:

$$P_{\{+,x\}} = c_{\{0,+,x\}} + c_{\{1,+,x\}}\, t + c_{\{2,+,x\}}\, t^2 + c_{\{3,+,x\}} t^3 \qquad \textit{Eq 4}$$

The other position polynomials, $P_{\{\text{♁},y\}}$, $P_{\{\text{♁},z\}}$, $P_{\{+,y\}}$ and $P_{\{+,z\}}$ are determined accordingly. The next step is to subtract the Earth and asteroid polynomials corresponding to each Cartesian component. This is demonstrated here for the x component:

$$P_{\{\text{♁}+,x\}} = P_{\{\text{♁},x\}} - P_{\{+,x\}} \qquad \textit{Eq 5}$$

$$P_{\{\text{♁}+,x\}} = \left(c_{\{0,\text{♁},x\}} - c_{\{0,+,x\}}\right) + \left(c_{\{1,\text{♁},x\}} - c_{\{1,+,x\}}\right) t + \left(c_{\{2,\text{♁},x\}} - c_{\{2,+,x\}}\right) t^2 + \left(c_{\{3,\text{♁},x\}} - c_{\{3,+,x\}}\right) t^3 \qquad \textit{Eq 6}$$

In accordance with Pythagoras, the difference polynomials for each component were squared and summed to produce the square of the distance, $D_{\{\text{♁}+\}}$, between the Earth and the asteroid:

$$D^2_{\{\text{♁}+\}} = P^2_{\{\text{♁}+,x\}} + P^2_{\{\text{♁}+,y\}} + P^2_{\{\text{♁}+,z\}} \qquad \textit{Eq 7}$$

The result of this computation is $D^2_{\{\text{♁}+\}}$ and is a polynomial in itself. To find the time of impact of the asteroid, the real roots of Eq 7 are determined after the distance $D_{\{\text{♁}+\}}$ is set equal to Earth's radius (6371 km) plus 42 km to model the surface of the atmosphere. In general, more than one real root can be found. One root is the time when the asteroid penetrates the sphere (6413 km radius) of the Earth, this is the impact time, and another root is the time when the asteroid exits the sphere of the Earth. Additional roots may be found that depend on the polynomial behavior outside the time interval of interest in the vicinity of the impact time. To determine the correct real root, the time of closest approach is considered. The time of closest approach

is found by differentiating Eq 7 with respect to time. The first derivative of Eq 7 evaluates to zero at the time of closest approach. The correct time of impact is the real root closest to the time of closest approach that is also smaller than the time of closest approach. The time of impact serves as input to the positional polynomials of the asteroid ($P_{\{+,x\}}, P_{\{+,y\}}$ and $P_{\{+,z\}}$) to obtain the precise impact coordinates. The obtained impact time determines the sidereal hour angle of the Earth [15] which, together with the impact coordinates, allows calculation of the impact's latitude and longitude. This is the impact point of the VI solution.

Orbit solutions that are located in the immediate vicinity of the VI and on its LOV also impact the Earth. To construct the impact corridor, the LOV is sampled by varying the epoch associated with the VI's orbital solution. The sampled orbit solutions produce impact points that form the impact corridor together with the impact point of the VI. Sampling by varying the VI's orbit solution epoch is equivalent to assuming that the LOV stretches in a similar direction as the VI's velocity vector. In the "vast majority of cases" this is a reasonable assumption [10] and the calculated impact corridor will match the real impact corridor.

To validate the impact corridor calculation of the ARMOR tool, three case studies were selected representing asteroids 2011AG5, 2008TC3 and 2014AA. In the case of 2011AG5 successful cross-validation with other predictive software tools was accomplished. Additional details on this case are provided in [16].

Asteroid 2008TC3 was discovered shortly before entering the Earth's atmosphere. Its entry point was predicted and the resulting bolide was observed by eye witnesses, satellite and infra-sound sensors [17,18]. For validation, ARMOR used the nominal orbital solution for 2008TC3 and predicted the atmospheric entry point as well as the ground track (Figure 2). The predicted nominal entry point agreed to within 0.39º longitude and 0.12º latitude (corresponding to a positional discrepancy of 44.3 km) at 65.4 km altitude. Furthermore, the shape of the ground track agreed well with the literature.

Similarly to 2008TC3, asteroid 2014AA was discovered a few hours before its collision with the Earth. Based on the available observations, the entry point could be constrained to lie in the southern Atlantic Ocean. With the help of a global network of infra-sound microphones that recorded and triangulated the impact event, a the most likely impact location was determined at the coordinates 44.207º longitude west and 13.118º latitude north [19]. ARMOR predicted the entry point corresponding to the nominal, best fit orbit solution, provided by HORIZONS, at 46.42º longitude west and 12.98º latitude north. This corresponded to a discrepancy of about 240.2 km (with most of the deviation along the line of variation) and the result is shown in Figure 3.

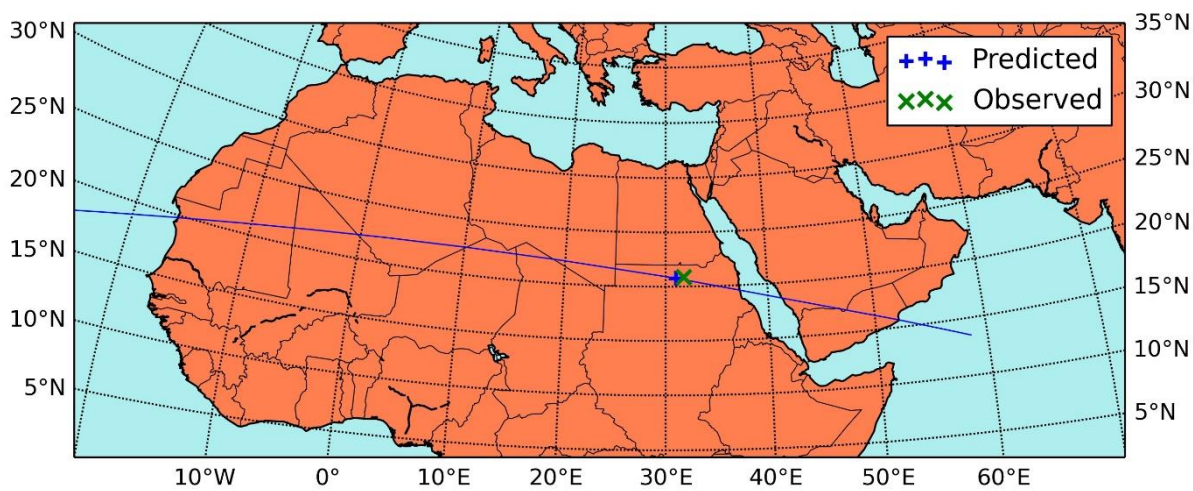

Figure 2: Observed and predicted entry point for asteroid 2008TC3. The blue plus sign marks the point of the nominal entry solution while the green cross gives the solution of the observed entry point at the same altitude of 65.4 km.

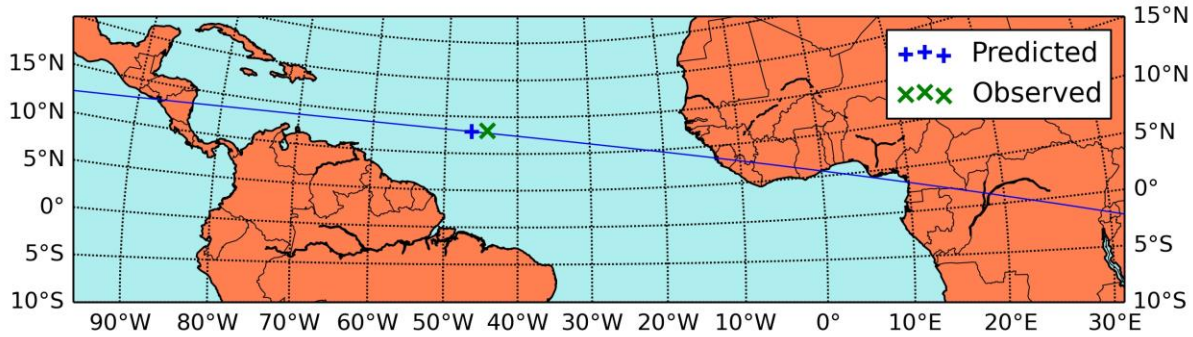

Figure 3: Observed and predicted entry point for asteroid 2014AA. The blue plus sign marks the point of the nominal entry solution while the green cross gives the solution of the observed entry point at the same altitude of 50 km.

The positional discrepancy between observed and predicted impact points can be explained by several factors. The asteroid ephemeris is not known perfectly and the real and propagated trajectories differ through this error in the initial conditions. The propagator has an inherent propagation error that results in a deviation from the real trajectory. ARMOR uses a spherical Earth model (radius = 6371 km) and does not presently account for the oblateness of the Earth. This means that the impact location is effectively calculated at a different altitude than the observed one. Given a non-perpendicular impact trajectory with respect to the local horizon, the difference in altitude will produce a position error in the horizontal plane. Furthermore, ARMOR does not account for atmospheric interaction in the trajectory calculation while a real asteroid will experience drag and lift forces during atmospheric entry. The aerodynamic forces affect the flight path of the asteroid. It is also expected that thermo-chemical interactions such as ablation and the resulting mass loss affect the asteroid trajectory and these effects are not modelled in ARMOR. Given the modelling constraints of ARMOR, the predicted impact points are reasonably close to the observed ones and the validation cases demonstrate that the impact point and corridor line calculations produce plausible results.

The impact corridor line forms the center line of the impact probability corridor projected on the Earth. A normal distribution with a 1-sigma value equal to the LOV width (a parameter available on the NEO webpages) is centered on the impact corridor line to represent the cross track impact probabilities. This newly formed impact probability distribution is scaled so that its integral is equal to the impact probability of the VI. The global impact probability of a VI is provided by OrbFit and can also be checked on one of the NEO webpages.

II.II IMPACT EFFECTS

Modelling of impact effects and estimation of casualties is the most recent addition to ARMOR and all impact effect modelling is directly derived from the "Earth Impact Effects Program" [20]. Six physical impact effects are modelled and the occurrence of each effect depends on the fate that an asteroid awaits upon collision with the Earth. While passing through the atmosphere, smaller asteroids are prone to undergo rapid disintegration in an explosion-like event called airburst [21]. In this case, an aerodynamic wave that generates a wind gust and overpressure shock propagates away from the airburst location. The airburst also emits thermal radiation that can burn surfaces which are impinged. Bigger asteroids can pass the atmosphere intact and produce a crater upon land impact. The cratering process itself as well as the accompanying out throw of ejecta account for two additional impact effects while the ground impact provoked seismic shaking adds the last. Similarly to an airburst, the cratering event produces wind gust, overpressure and thermal radiation.

Notably, tsunamis were not part of the analysis because tsunami model implementation was not completed at the time this publication was produced. However, this circumstance helps to preserve comparability between the previous and current results. In previous results, only direct land impacts have been modelled because no effect propagation was performed due to the lack of impact effect models and thus, only the population that lives in the impact map cell could be considered for risk calculation. The oceans are uninhabited and those map cells would therefore not contribute to the risk calculation. Furthermore, while it is true that all impact effects propagate beyond their impact point, tsunamis stand out because their reach is significantly farther than any of the other effects [6]. Because of the

far reach of tsunamis and because populations show concentrations in coastal regions, this effect could be one the most dominant of all effects. Ocean impacts would be expected to contribute significantly to risk outcomes in the newer results while they were unaccounted for in previous results. This would have the effect of pronouncing coastal areas in the risk assessment in a way that is a clear deviation from the method that was used to obtain previous. Excluding tsunamis allows the focus on the comparison of risk assessment for direct land impacts with and without physical impact effects.

II.III RISK

Risk of a map cell (R_c) is defined here as the product of the probability of an asteroid impact in a specific cell (ρ_c), the number of people that lives in the area which is exposed to the impact generated effects (Ψ) and the vulnerability of the exposed population (η) to the impact effects which are attenuated by distance to the impact site.

$$R_c = \rho_c \times \Psi \times \eta$$

Vulnerability of the population depends on the severity of impact effects and severity describes how powerful each effect is at a given distance. Very strong impact effects (e.g. magnitude 8 equivalent seismic shaking) cause more casualties and, thus, vulnerability is high while a moderate tremor (e.g. magnitude 4 seismic shaking) leaves the population mostly unharmed and resulting in low vulnerability.

In the previous impact risk analysis, which did not account for physical impact effects, vulnerability (η) was set equal to one because the simulation was incapable of calculating the severity and extent of impact effects. Instead, it was assumed that the impact cell's population is equal to the number of casualties. Risk, in this case was the product of impact cell population times probability of impact in that cell. The new results account for physical impact effects and, consequently, vulnerability is a function of severity. Furthermore, the attenuation of impact effects with distance is modelled which allows the count of the population in affected cells beyond the impact cell and also to vary vulnerability as impact effects propagate into more distant cells and weaken.

Finally, the national risk of all countries is determined by summing the risk distribution within each country's borders. The national risk values are divided by the global risk to produce the percentage of global risk that each country faces and this is called the relative risk of a nation. The formula for relative risk in each map cell is:

$$\text{relative risk}_c = \sum_{i}^{261} \frac{R_{i,c}}{\sum_c \mathrm{R_{i,c}}} \qquad \textit{Eq 8}$$

III. RESULTS

The results are based on 69 known asteroids that produce 261 VIs and these asteroids were sampled in the November 2014 timeframe. All 261 Vis were subjected to the method described above and the first result is a set of impact corridors, each in the form of a Gaussian distribution that reflects the impact probabilities of the assessed VIs. All impact solutions were combined within a global map and the global impact probability distribution is shown in Figure 4. Based on the individual probability corridors in this map, the impact probability in each map cell and for each VI could be determined for subsequent risk calculation.

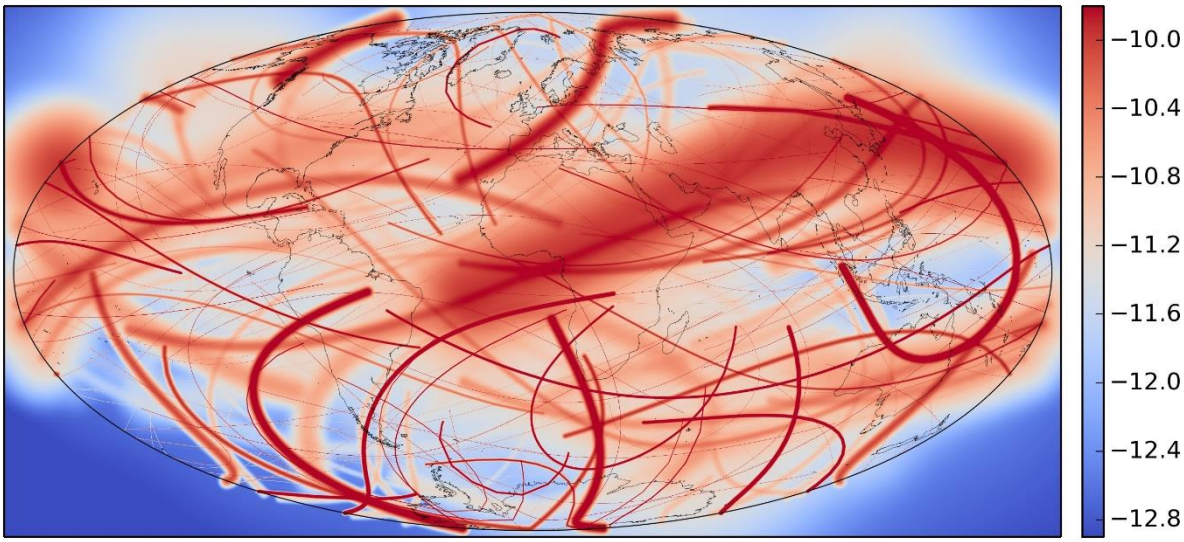

Figure 4: The Earth in the Hammer projection showing the impact probability distributions for 261 VIs. The colour coding represents the impact probability at each location using a logarithmic scale (shown right).

By means of combining Figure 4 with the world population, the global risk distribution without consideration for physical impact effects is produced. This is the "old" risk distribution and it is shown in Figure 5. A discussion of the results that are based on this figure can be found in the dedicated Planetary Defense Conference paper [9].

The purpose of this paper is to discuss the effect that the introduction of physical effects has into the risk distribution. To this end, the global asteroid risk distribution has been recalculated considering impact effects and the new risk distribution is shown in Figure 6. Noticeable differences between Figure 5 and Figure 6 are that some individual asteroid corridors disappear and new ones become more pronounced because they correspond to higher energy impacts (larger asteroids) that raise the risk in the areas that are crossed by these corridors. Furthermore, the risk landscape extends beyond continental territory and beyond the shores of islands because physical effects of near coastal impacts propagate onto the land (aerodynamic shockwaves and thermal radiation).

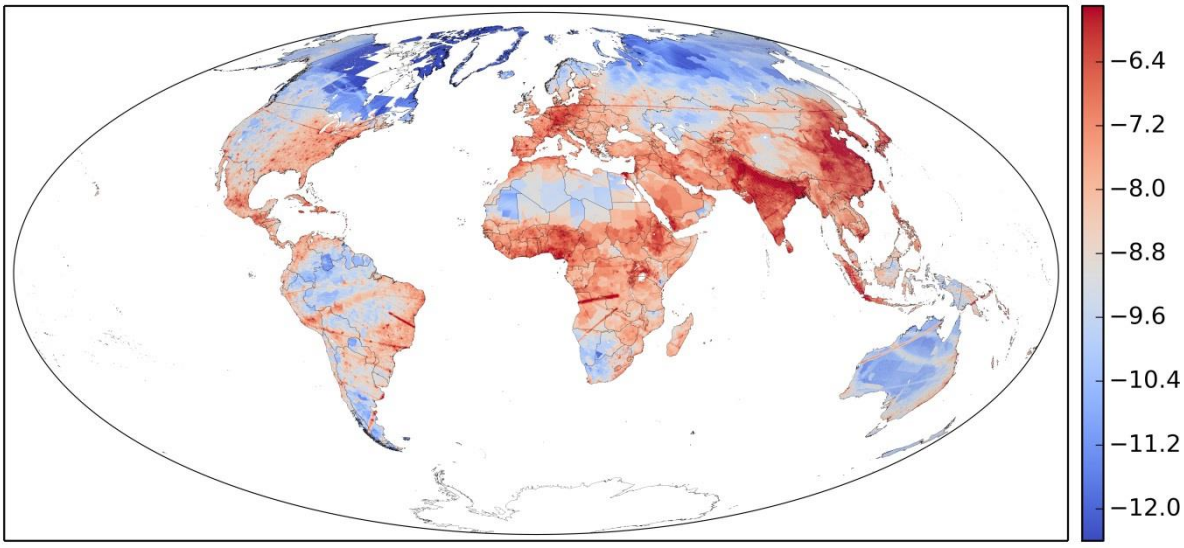

Figure 5: The "old" asteroid risk map is a combination of impact probability and world population data but does not account for physical impact effects. The colour in each region indicates the risk level for that population. Risk is normalized with respect to global risk and is colour coded using a logarithmic scale.

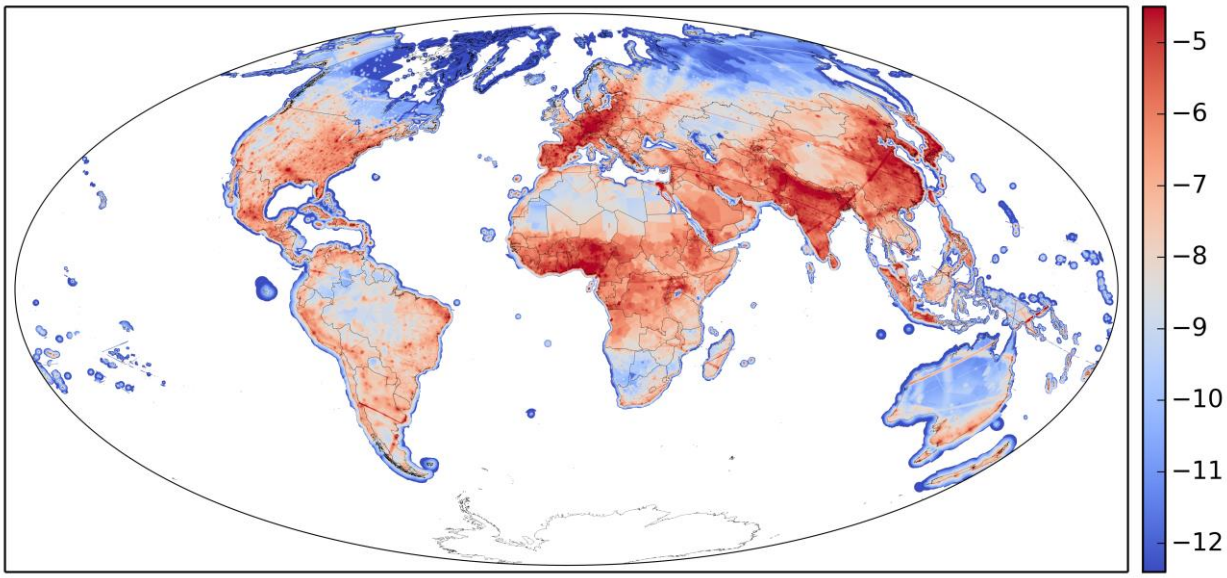

Figure 6: The "new" asteroid risk map combines impact probability, exposed population and the vulnerability of that population based on physical impact effect calculation. The colour in each region indicates the risk level for that population. Risk is normalized with respect to global risk and is colour coded using a logarithmic scale.

Finally, the national risk list based on risk results with and without physical impact effects is produced for quantitative analysis of changes in global risk distribution. Figure 7 shows the risk list and also includes the relative global population share that each nation hosts. The data is sorted in descending order by population size of the 40 most populous nations. It appears that population size is a good proxy for risk. In fact, national population size and risk values share a correlation coefficient of 0.953 in the case of the old results and 0.907 in the case of the new results.

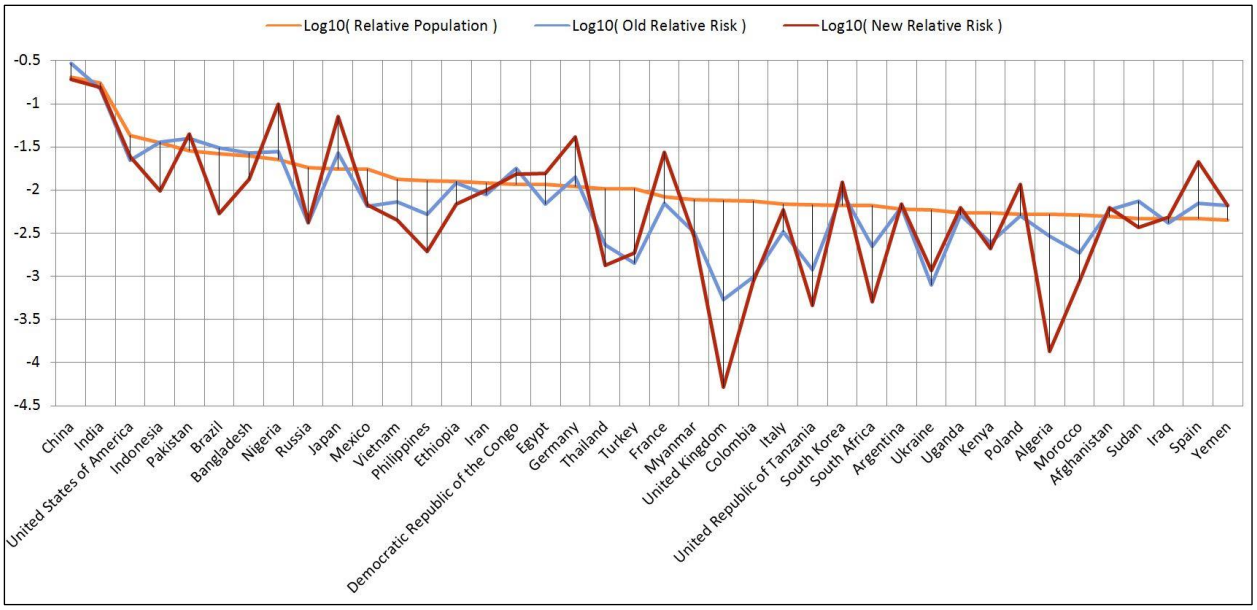

Figure 7: National risk list for the 40 most populous countries. Risk data is based on old data that does not account for physical impact effects and for new data that accounts for those effects. Both datasets focus on direct land impacts (and near coastal impacts in the case of the new results). The data is presented on a logarithmic scale and based on relative values that express the global share of risk and population accredited to each nation.

The results that are shown here are constrained to impacts that occur over land, only.

IV. DISCUSSION

The first, general observation that can be made based on the data shown in the risk list (Figure 7) is that population size is a decent proxy for national direct asteroid impact risk. The risk data share high correlation coefficients with population data of 0.953 and 0.907 in the cases without and with impact effects, respectively. The inclusion of physical impact effects did not have a major impact on this rule of thumb. This assessment is further supported by visual inspection of the global risk distribution maps of Figure 5 and Figure 6. While the appearance of individual impact corridors varies, broader, high risk areas remain constant such as central Africa, India, China's coastal region and central Europe.

The close correlation of population density with direct impact risk distribution stems from the generally recognised assumption that over timescales measured in tens of years, the impact distribution of asteroids on Earth is uniform. If all asteroids had the same impact probability, the impacts in this work would also be uniformly distributed. If, additionally, impact effects, would be disregarded, as has been done in the old results, the risk distribution would mirror the population distribution perfectly. Consequently, the variation between population and risk data in the old results is a function of individual impact probabilities of the VIs. Impact probabilities account for the deviation that results in a correlation coefficient of 0.953 (instead of 1) between population and impact effects. Markedly, the disregard for physical impact effects ignores the fact that the analysed asteroids differ in size and impact speed. Instead, all impacts have been treated equally by assuming that the population in the impact map cell would be counted as casualties.

With the inclusion of physical impact effects the latter assumption of equal impact consequences (effectively disregarding physical properties of each asteroid such as size and speed) is corrected. A risk increase in the new results reflects that this nation happens to be affected by a high energy impact while a decrease means that this nation happens to be primarily affected by low energy impacts with little consequences. Through the inclusion of physical impact effects, additional complexity is added to the analysis because the analysed asteroids differ in size and impact speed and risk results vary accordingly. Consequently, the new risk result reflects this additional complexity in further discrepancy between population density and risk. Noticeably, the correlation coefficient decreases to 0.907. This finding is confirmed in the risk list of Figure 7 where risk numbers that consider impact effects deviate further from population marks than those disregarding physical impact effects.

The increase in variation due to the inclusion of impact effects is moderate as expressed by the decreasing correlation coefficient (only 4.8% with respect to previous results) and might be weaker than expected. This outcome can be partially ascribed to the lack of tsunami modelling. It is expected that nations with a disproportionately long coastline relative to their country size would accumulate higher risk values since tsunamis are supposed to contribute significantly to potential asteroid impact casualty counts [22].

Figure 7 is ordered by population size. In reference [9], a similar list is sorted by decreasing risk presenting the 40 countries that experience highest risk based on results that do not account for impact effects. The inclusion of impact effects caused a substantial reshuffling in the risk ranking. Brazil, for instance, dropped by 32 positions from 5 to 37 (in a list of 206 countries). On the other hand, Russia climbed by 9 positions from 37 to 28. The median position change in the 40 most populated countries was 9.5 ranks. These findings show that models that account for impact effects are required in order to make accurate predictions about which specific countries face a specific risk because predictions that are based on impact probability and population alone only produce moderately accurate estimates in this respect. While the assertion that population size serves as proxy for asteroid risk remains true when considering the equally distributed background risk of asteroid impacts, analysis that includes physical impact effects as well as a spatial distribution of impact locations is needed to determine proper risk levels for individual countries.

The asteroid lists maintained by ESA and NASA change over time with the discovery of new high impact probability asteroids and the exclusion of asteroids that were previously considered with a high impact probability. New observations will also adjust the impact probability of asteroids already present in the lists and, thus, the risk landscape will change. Only about 1% of all Near Earth Asteroids have been observed [23]. The majority, especially in the sub-km size regime, have yet to be discovered. Consequently, the results shown here represent only a snapshot in time of knowledge of the asteroid hazard. However, the conclusions drawn based on this snapshot data

will likely hold true in the future even if the risk landscape changes.

The results highlight the fact that each nation on Earth could potentially be impacted by an asteroid and its population could be harmed. For all countries, efficient preparation for a potential impact means increasing public awareness and including the asteroid hazard in natural disaster response planning. Disaster response planning should address direct impact effects such as blast waves, hot thermal radiation and seismic shocks. For example, the Chelyabinsk bolide generated a shockwave that shattered windows and the glass shards injured people standing nearby. A pre-disaster plan that warns people to seek shelter and to avoid windows at the time of atmospheric passage would be an effective way to protect the population in the case of a bolide airblast close to an urban area.

CONCLUSIONS

This paper addresses the question of how the inclusion of physical impact effects changes the risk landscape with respect to previous results that did not account for physical impact effects. The impactor sample is made up of impact corridor and probability distributions of 261 VIs belonging to 69 asteroids that currently have a chance of colliding with the Earth. The distributions are calculated and visualized using the ARMOR software tool that can project impact probabilities of known asteroids onto the surface of the Earth. ARMOR's method was outlined and validation cases for its propagation accuracy as well as impact point and corridor calculation were presented. In this respect, the validation cases demonstrated that the tool produces plausible results. In addition, an analytical approach was developed to find the asteroid's impact point and time.

The results show that the risk landscape changes moderately with the inclusion of physical impact effects. The observation from previous results that population size is a suitable proxy for national risk remains valid after the introduction of impact effects. The relationship between population size and relative risk weakens by 4.8% compared to previous results which reflects in a decrease of the population-risk correlation coefficient from 0.953 to 0.907. The reason for the correlation decrease is that physical impact effects add complexity to the analysis that yields greater variation in the results. As a rule of thumb population size helps to estimate national risk, but high impact probability asteroids or large asteroids can significantly alter that image. Therefore, when considering the abstract background threat of asteroids, population size serves as a proxy to identify those countries that would suffer most casualties. However, when facing a concrete threat, population size is insufficient to identify which country is most at risk and detailed analysis is needed in this case.

ACKNOWLEDGEMENTS

The work is supported by the Marie Curie Initial Training Network Stardust, FP7-PEOPLE-2012-ITN, Grant Agreement 317185. Peter Atkinson is grateful to the University of Utrecht for supporting him with The Belle van Zuylen Chair.

REFERENCES

1. Wetherill, G. W. Formation of the Earth. *Annu. Rev. Earth Planet. Sci.* **18,** 205–256 (1990).

2. Ryder, G. Mass flux in the ancient Earth-Moon system and benign implications for the origin of life on Earth. *J. Geophys. Res.* **107,** (2002).

3. Alvarez, L. W., Alvarez, W., Asaro, F. & Michel, H. V. Extraterrestrial cause for the cretaceous-tertiary extinction. *Science (80-.).* **208,** 1095–1108 (1980).

4. Popova, O. P. *et al.* Chelyabinsk airburst, damage assessment, meteorite recovery, and characterization. *Science* **342,** 1069–73 (2013).

5. Chyba, C. F., Thomas, P. J. & Zahnle, K. J. The 1908 Tunguska explosion: atmospheric disruption of a stony asteroid. *Nature* **361,** (1993).

6. National Research Council *et al. Defending Planet Earth : Near-Earth Object Surveys and Hazard Mitigation Strategies*. (2010).

7. Universita Di Pisa & European Space Agency. NEODyS-2 Risk Page. (2014). at <http://newton.dm.unipi.it/neodys/index.php?pc=4.1>

8. NASA. NASA NEO Impact Risk. (2014). at <http://neo.jpl.nasa.gov/risk/>

9. Rumpf, C., Lewis, H. G. & Atkinson, P. M. GLOBAL IMPACT DISTRIBUTION OF ASTEROIDS AND AFFECTED POPULATION. in *IAA Planet. Def. Conf.* (2015). at <http://eprints.soton.ac.uk/377825/>

10. Milani, A., Chesley, S. R., Sansaturio, M. E., Tommei, G. & Valsecchi, G. B. Nonlinear impact monitoring: line of variation searches for impactors. *Icarus* **173,** 362–384 (2005).

11. Milani, A. *et al.* The OrbFit Software Package. *GNU Gen. Public Licens.* (1997). at <http://adams.dm.unipi.it/orbfit/>

12. Folkner, W. M., Williams, J. G., Boggs, D. H., Park, R. S. & Kuchynka, P. *The Planetary and Lunar Ephemerides DE430 and DE431*. (2014). at <http://ipnpr.jpl.nasa.gov/progress_report/42-196/196C.pdf>

13. Radhakrishnan, K. & Hindmarsh, A. C. *Description and Use of LSODE, the Livermore Solver for Ordinary Differential Equations*. (1993). at <http://hdl.handle.net/2060/20050186722>

14. Giorgini, J. & Yeomans, D. K. *Horizons (Version 3.75). Jet Propuls. Lab.* (Jet Propulsion Laboratory, 2013). at <ftp://ssd.jpl.nasa.gov/pub/ssd/Horizons_doc.pdf>

15. Curtis, H. D. *Orbital Mechanics for Engineering Students*. (Elsevier Butterworth-Heinemann, 2012).

16. Rumpf, C. Global Asteroid Risk Analysis. in *Int. Astronaut. Congr. 2014* 1–10 (2014). doi:10.13140/2.1.3739.5208

17. Jenniskens, P. *et al.* The impact and recovery of asteroid 2008 TC3. *Nature* **458,** 485–8 (2009).

18. Chesley, S. R., Chodas, P. W. & Yeomans, D. K. Asteroid 2008 TC3 Strikes Earth: Predictions and Observations Agree. *NASA Near Earth Object Progr.* 1–6 (2014). at <http://neo.jpl.nasa.gov/news/2008tc3.html>

19. Chesley, S. R., Farnocchia, D., Brown, P. G. & Chodas, P. W. Orbit Estimation for Late Warning Asteroid Impacts: The Case of 2014 AA. in *IEEE Aerosp. Conf.* 1–8 (IEEE, 2015). at <http://ieeexplore.ieee.org/xpl/articleDetails.jsp?arnumber=7119148>

20. Collins, G. S., Melosh, H. J. & Marcus, R. a. Earth Impact Effects Program: A Web-based computer program for calculating the regional environmental consequences of a meteoroid impact on Earth. *Meteorit. Planet. Sci.* **40,** 817–840 (2005).

21. Boslough, M. & Crawford, D. a. Low-altitude airbursts and the impact threat. *Int. J. Impact Eng.* **35,** 1441–1448 (2008).

22. Bailey, N. J., Swinerd, G. G., Lewis, H. G. & Crowther, R. Global vulnerability to near-Earth object impact. *Risk Manag.* **12,** 31–53 (2010).

23. Harris, A. W. & D'Abramo, G. The population of near-earth asteroids. *Icarus* (2015). doi:10.1016/j.icarus.2015.05.004